Original Article

Value of mammographic microcalcifications and MRI-enhanced lesions in the evaluation of residual disease after neoadjuvant therapy for breast cancer

Chao Zhu[1,2,3#], Minglei Chen[1,2,4#], Yulin Liu[1,2#], Pinxiong Li[1,2], Weitao Ye[1,2], Huifen Ye[1,2], Yunrui Ye[1,2], Zaiyi Liu[1,2], Changhong Liang[1,2*], Chunling Liu[1,2*]

[1]Department of Radiology, Guangdong Provincial People's Hospital (Guangdong Academy of Medical Sciences), Southern Medical University, Guangzhou, China; [2]Guangdong Provincial Key Laboratory of Artificial Intelligence in Medical Image Analysis and Application, Guangzhou, China; [3]Department of Radiology, Ningyuan County People's Hospital, Yongzhou, China; [4]Shantou University Medical College, Shantou, China

Contributions: (I) Conception and design: C Zhu, M Chen, Y Liu; (II) Administrative support: C Liang, C Liu; (III) Provision of study materials or patients: Z Liu; (IV) Collection and assembly of data: H Ye, Y Ye; (V) Data analysis and interpretation: P Li, W Ye; (VI) Manuscript writing: All authors; (VII) Final approval of manuscript: All authors

[#]These authors contributed equally to this work.

[*]These authors contributed equally to this work as co-corresponding authors.

Correspondence to: Changhong Liang, MD; Chunling Liu, MD. Department of Radiology, Guangdong Provincial People's Hospital (Guangdong Academy of Medical Sciences), Southern Medical University, No. 106 Zhongshan Er Road, Guangzhou 510080, China; Guangdong Provincial Key Laboratory of Artificial Intelligence in Medical Image Analysis and Application, Guangzhou, China. Email: liangchanghong@gdph.org.cn; liuchunling79@163.com.

Background: Microcalcifications persist even if a patient with breast cancer achieves pathologic complete response (pCR) as confirmed by surgery after neoadjuvant treatment (NAT). In practice, surgeons tend to remove all the microcalcifications. This study aimed to explore the correlation between changes in the extent of microcalcification after NAT and pathological tumor response and compare the accuracy of mammography (MG) and magnetic resonance imaging (MRI) in predicting the size of residual tumors.

Methods: This was a retrospective study which included a consecutive series of patients in Guangdong Provincial People's Hospital. Between January 2010 and January 2020, 127 patients with breast cancer and Breast Imaging Reporting and Data System (BI-RADS) 4–5 microcalcifications were included in this study. The maximum diameter of the microcalcifications on MG and lesion enhancement on MRI pre- and post-NAT were measured. The correlations between the changes in residual microcalcifications on MG and pCR were analyzed. Intraclass correlation coefficients (ICCs) were computed between the extent of the residual microcalcifications, residual enhancement, and residual tumor size.

Results: There were no statistically significant differences in the changes in microcalcifications after NAT according to the RECIST criteria on MRI (P=0.09) and Miller-Payne grade (P=0.14). MRI showed a higher agreement than did residual microcalcifications on MG in predicting residual tumor size (ICC: 0.771 *vs.* 0.097).

Conclusions: MRI is more accurate for evaluating residual tumor size in breast cancer. In our study, the extent of microcalcifications on MG after NAT had nearly no correlation with the pathological size of the residual tumor. Therefore, residual tumors with microcalcifications may not necessarily be a contraindication to breast-conserving surgery.

Keywords: Breast neoplasms; mammography (MG); magnetic resonance imaging (MRI); neoadjuvant therapy; microcalcifications

Submitted Oct 27, 2022. Accepted for publication Jul 17, 2023. Published online Aug 11, 2023.
doi: 10.21037/qims-22-1170
View this article at: https://dx.doi.org/10.21037/qims-22-1170

Introduction

Breast cancer has become the foremost leading cancer worldwide (1). Approximately 30–50% of cases of nonpalpable breast cancer are detected by mammogram scans alone due to the appearance of microcalcifications (2-4). Neoadjuvant treatment (NAT) has proven effective in reducing tumor size, thus enabling surgical intervention for initially inoperable patients (5). Accurate assessment of residual tumor size after NAT is vital for surgical planning (6). However, even if the tumor exhibits pathologic complete response (pCR) after NAT, microcalcifications can remain on mammography (MG) (7). The removal of all residual microcalcifications after NAT remains controversial (8). According to the guidelines set forth by the National Comprehensive Cancer Network (NCCN), diffuse malignant calcification is an absolute contraindication for breast-conserving surgery (BCS) (9). In modern clinical practice, surgeons tend to remove all calcifications (10); however, this approach may potentially exclude certain patients with persistent microcalcifications who have achieved pCR, thus limiting their eligibility for breast conservation therapy. In order to develop individualized treatment plans, accurate evaluation of the residual lesion size after NAT is essential. Hence, this study aimed to investigate the correlation between changes in microcalcifications pre- and post-NAT as well as the relationship between pCR and these changes. Additionally, the study aimed to compare the accuracy of MG and magnetic resonance imaging (MRI) in evaluating the size of residual tumors. We present this article in accordance with the STROBE reporting checklist (available at https://qims.amegroups.com/article/view/10.21037/qims-22-1170/rc).

Methods

Patients

The study was conducted in accordance with the Declaration of Helsinki (as revised in 2013) and was approved by the Research Ethics Committee of Guangdong Provincial People's Hospital. Individual consent for this retrospective analysis was waived.

We retrospectively reviewed all patients with pathologically confirmed breast cancer with microcalcifications who underwent NAT prior to surgery at our hospital between January 2010 and January 2020. The inclusion criteria were as follows: (I) MG showing BI-RADS 4–5 microcalcifications before NAT, but microcalcifications not appearing on MRIs; and (II) both MG and MRI examinations performed before and after NAT. The exclusion criteria were as follows: (I) previous history of breast cancer or surgery; (II) presence of distant metastases at the time of diagnosis; (III) absence of pathological tumor data or other necessary pathological information; and (IV) poor image quality. The flowchart of patient inclusion is shown in *Figure 1*.

MG and MRI examinations

MG and MRI examinations were performed on all patients before and after the NAT. Standard MG was performed using 1 of 2 scanners (Hologic Selenia Dimensions or uMammo590i). Craniocaudal and mediolateral oblique views were obtained for all patients.

Two different MRI scanners with a 1.5 T system (Optima 360, GE HealthCare, USA; Achieva, Philips Medical System, The Netherlands) were used, with a dedicated breast coil for patients in the prone position.

The GE/Philips sequence scan parameters were as follows: (I) T1-weighted sequence: repetition time =5.8/4.8, echo time =2.7/2.1, acquisition matrix =330/300×330/320, and thickness =2/2 mm; (II) fat-suppressed T2-weighted sequence: repetition time =5,045/3,400, echo time =102/90, acquisition matrix =320/320×320/260, and thickness =3/3 mm; (III) axial diffusion-weighted sequence (DWI): b values =0/0 or 1,000/1,000 s/mm^2; and (IV) dynamic contrast material-enhanced (DCE) MRI sequence scan parameters: axial data obtained with repetition time =5.1/5.1 ms, echo time =2.3/2.2 ms, flip angle =10°, acquisition matrix =320/320×320/300, pixel size =1.00 mm × 1.00 mm, number

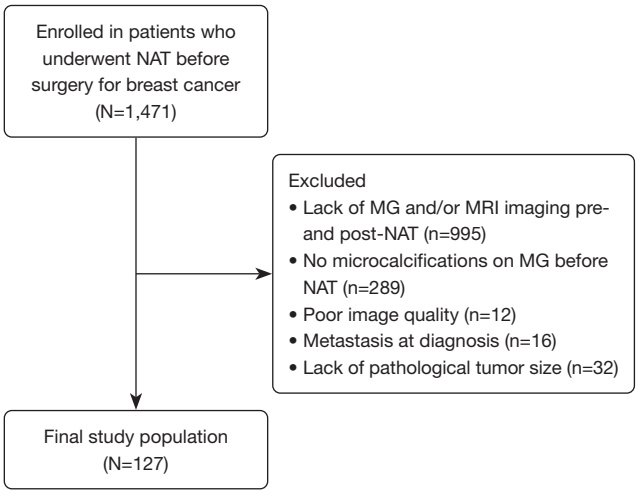

Figure 1 Flowchart of patient inclusion and exclusion. NAT, neoadjuvant treatment; MG, mammography; MRI, magnetic resonance imaging.

of excitations =1, and slice thickness =2.0/1.0 mm. The first enhanced sequence image acquisition was started 25 s after the contrast agent was injected. The acquisition was repeated 6 times, and each phase lasted 75/60 s. Both DCE-MRI types involved the automatic injection of the contrast agent (gadopentetate dimeglumine; BeiLu Healthcare; 0.2 mL/kg body weight, flow rate 1.5 mL/s) and then flushing with the same total dose of saline solution.

Image analysis

All images were reviewed retrospectively by 2 radiologists with 5 and 15 years of experience in breast imaging who arrived at a consensus. MG findings were assessed using the BI-RADS classification system (11). On each mammogram, the morphology and distribution of microcalcifications before and after NAT were recorded together with the largest extent of microcalcifications in the craniocaudal and mediolateral oblique views. After NAT, the calcification extent was considered to increase if the calcification diameter increased by ≥10% compared with that before treatment; if the calcification range decreased by ≥10% compared with that before treatment, the calcification range was considered to be reduced; and if the calcification range after treatment was between the increase and decrease, the extent of calcification was considered unchanged.

On DCE-MRI, the greatest tumor diameter before or after NAT was measured as the tumor size in early post-contrast imaging. In the case of multiple lesions, the largest tumor was used to define the tumor size. The response evaluation on MRI was based on the revised Response Evaluation. Criteria in Solid Tumors (RECIST) guidelines (version 1.1) (12). Complete response was defined as the disappearance of any residual mass or non–mass enhancement, partial response was defined as a decrease of >30% in the greatest diameter, progressive disease was defined as an increase of >20% in the greatest diameter, and stable disease was defined as an increase of <20% or a decrease of <30% in the largest diameter.

Histopathology analysis

Surgery was performed after the completion of NAT. Pathological tumor size was recorded. The main biomarkers, estrogen receptor (ER), progesterone receptor (PR), and human epidermal growth factor receptor 2 (HER2) were assessed using immunohistochemistry (IHC) in paraffin-embedded tumor samples before treatment. Patients were categorized based on the IHC hormone receptor (HR) and HER2 status of their primary tumor. Therefore, the tumor subtypes were classified as follows: (I) HR-negative/HER2-positive (ER-negative, PR-negative, and HER2-positive); (II) HR-positive/HER2-positive (ER-positive and/or PR-positive, and HER2-positive); (III) HR-positive/HER2-negative (ER-positive and/or PR-positive, and HER2-negative); and (IV) triple-negative (TN) (ER-negative, PR-negative, and HER2-negative) (13). Histopathological tumor response was assessed using the Miller-Payne (MP) grading system (14). MP grade V and residual ductal carcinoma in situ (DCIS) were included in the pCR category (6).

Statistical methods

SPSS 26.0 (IBM, Armonk, NY, USA) was used for the statistical analysis. Continuous, nonnormally distributed variables are expressed as median and interquartile range (IQR), and categorical variables as frequencies and percentages. Comparisons were performed using the Wilcoxon signed-rank test for nonnormally distributed continuous variables, and Pearson χ^2 test or Fisher exact test for categorical variables. The correlation between the extent of the residual microcalcifications on MG, the size of the residual enhancement on MRI, and the actual residual tumor size was assessed based on the intraclass correlation

Table 1 Baseline characteristics of all patients

Characteristic	Value
Age (years), mean ± SD	49.9±9.3
Neoadjuvant treatment regimen, n (%)	
Only neoadjuvant chemotherapy	65 (51.2)
Neoadjuvant chemotherapy + targeted therapy	60 (47.2)
Neoadjuvant chemotherapy + endocrine therapy	1 (0.8)
Neoadjuvant endocrine therapy + targeted therapy	1 (0.8)
Histological type before NAT, n (%)	
IDC	116 (91.3)
ILC	1 (0.8)
IDC + DCIS	10 (7.9)
Molecular subtype, n (%)	
HR–/HER2+	25 (19.7)
HR+/HER2+	42 (33.1)
HR+/HER2–	47 (37.0)
TN	13 (10.2)
pCR, n (%)	
Yes	52 (40.9)
No	75 (59.1)
Type of surgery, n (%)	
Breast-conserving surgery	24 (18.9)
Mastectomy	103 (81.1)
Pre-NAT tumor grade, n (%)	
1	5 (3.9)
2	74 (58.3)
3	48 (37.8)

SD, standard deviation; NAT, neoadjuvant treatment; IDC, invasive duct carcinoma; ILC, invasive lobular carcinoma; DCIS, ductal carcinoma *in situ*; HR, hormone receptor; HER2, human epidermal growth factor receptor 2; pCR, pathologic complete response; TN, triple negative.

coefficient (ICC). Sensitivity, specificity, positive predictive value (PPV), negative predictive value (NPV), false-positive rate, and false-negative rate of MRI were evaluated for diagnosing the residual tumor pCR. A two-tailed P value <0.05 was considered as to be statistically significant, and the confidence level of CIs was 95%.

Results

Patient clinicopathological characteristics

Clinicopathological features of the study population are described in *Table 1*. In total, 127 patients were enrolled in this study, and the mean patient age was 49.9±9.3 years. After NAT, 18.9% (24 of 127) of patients underwent BCS, and 81.1% (103 of 127) of patients underwent mastectomy (40 of 103 with pCR). In our study, 52 of the 127 patients (40.9%) achieved pCR after NAT. Among these, 19 of 52 (36.5%) were HR-negative/HER2-positive tumors, 21 of 52 (40.4%) were HR-positive/HER2-positive tumors, 8 of 52 (15.4%) were HR-positive/HER2-negative tumors, and 4 of 52 (7.7%) were TN tumors. There was a significant difference between tumor subtypes and pCR rates (P<0.001) (*Table 2*).

Mammographic findings

Table 3 shows the characteristics of microcalcifications. Fine pleomorphic (41.7%) and grouped distributions (51.2%) were the most common on pre-NAT MG. Among the 127 patients who underwent NAT, almost no changes were observed in the shape or distribution of microcalcifications. The shape of the microcalcifications changed in 2 patients, including 1 from coarse heterogeneous to amorphous, and 1 from fine pleomorphic to coarse heterogeneous. Only 1 case showed a change in distribution. A decrease in the extent of the microcalcifications was observed in 49 patients (38.6%), 22 (17.3%) patients showed increased calcification after treatment (*Figure 2*), and no interval change was observed in 56 (44.1%) patients. The median size of microcalcifications was 3.3 cm (IQR, 1.5–4.8 cm) before and 2.8 cm (IQR, 0.9–4.8 cm) after the NAT.

MRI findings

The median size of the tumor mass on MRI before and after NAT was 2.9 cm (IQR, 2.3–4.0 cm) and 0.8 cm (IQR, 0–1.5 cm), respectively. Among 42 patients who showed complete response on MRI (no residual enhancement in the tumor bed), 6 patients, all of who were ER-positive, failed to achieve real pCR. Sixteen patients showed enhanced lesions on MRI; however, the final pathological results indicated that they achieved pCR. The sensitivity, specificity, PPV, NPV, false-positive rate, and false-negative rate of MRI for

Table 2 Tumor subtype correlated with pathological reaction

pCR	Tumor subtype, n (%)				P value
	HR−/HER2+, n=25 (19.7)	HR+/HER2+, n=42 (33.1)	HR+/HER2−, n=47 (37.0)	TN, n=13 (10.2)	
Yes (n=52)	19 (36.5)	21 (40.4)	8 (15.4)	4 (7.7)	<0.001
No (n=75)	6 (8.0)	21 (28.0)	39 (52.0)	9 (12.0)	

pCR, pathologic complete response; HR, hormone receptor; HER2, human epidermal growth factor receptor 2; TN, triple negative.

Table 3 Mammography and MRI findings before and after NAT

Characteristic	Value
MG findings before NAT	
Lesion type	
Microcalcifications only	36 (28.3)
Microcalcifications with mass	91 (71.7)
Shape of microcalcifications	
Amorphous	21 (16.5)
Coarse heterogeneous	15 (11.8)
Fine pleomorphic	53 (41.7)
Fine linear/linear branching	38 (29.9)
Distribution of microcalcifications	
Scattered	2 (1.6)
Regional	14 (11.0)
Grouped	65 (51.2)
Segmental	44 (34.6)
Linear	2 (1.6)
Change in extent of microcalcifications	
Pre-NAT, cm	3.3 (1.5–4.8)
Post-NAT, cm	2.8 (0.9–4.8)
Changes in the shape and distribution of microcalcifications	
Fine pleomorphic—coarse heterogeneous	1 (0.8)
Coarse heterogeneous—amorphous	1 (0.8)
Cluster—scattered	1 (0.8)
MRI findings before NAT	
Lesion type	
Mass	103 (81.1)
Non-mass	24 (18.9)
Number of cancer lesions	
Single	76 (59.8)
Multiple	51 (40.2)
Tumor size pre-NAT, cm	2.9 (2.3–4.0)
Tumor size post-NAT, cm	0.8 (0–1.5)
Complete response on MRI after NAT	
Yes	42 (33.1)
No	85 (66.9)

Data are presented as n (%) or median (IQR). NAT, neoadjuvant treatment; MG, mammography; IQR, interquartile range; MRI, magnetic resonance imaging.

diagnosing residual tumor pCR were 92.0%, 69.2%, 81.2%, 85.7%, 30.8%, and 8.0%, respectively. MRI had the highest accuracy in evaluating whether HER2 overexpression and TN breast cancer exhibited pCR, with a sensitivity of 100% and a false-negative rate of 0%.

Correlation between change in the extent of microcalcifications and responses to NAT

The correlation between microcalcification extent change on MG after NAT, MRI radiologic reaction, and histopathologic characteristics are presented in *Table 4*. Of the 42 patients who achieved CR on MRI, microcalcifications decreased in 15 (35.7%) patients, and 22 (52.4%) showed no change in calcifications on MG (*Figure 3*). The change in microcalcifications was not significantly different according to the RECIST criteria (P=0.09). Similarly, there was no significant difference between the change in microcalcifications and the MP grade (P=0.14).

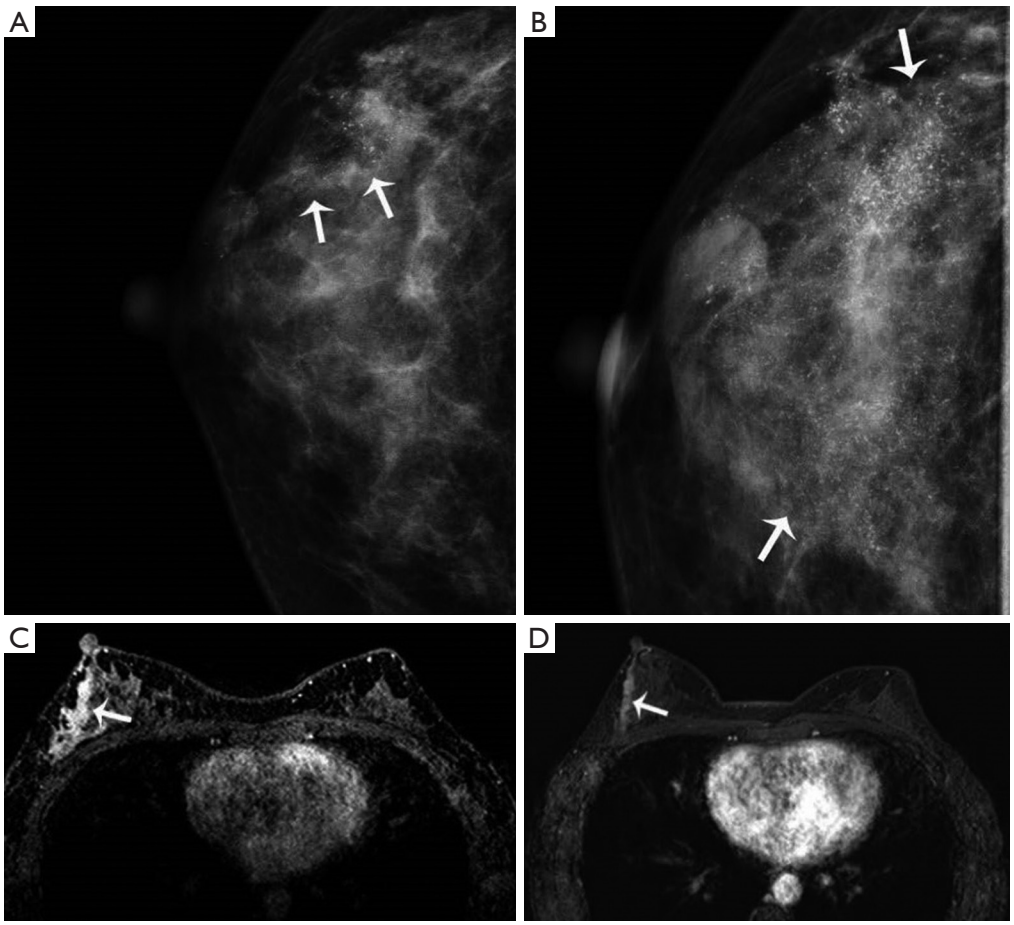

Figure 2 Imaging of a 42-year-old woman in whom a right breast lump was accidentally discovered. (A) Mammogram showing fine pleomorphic segmental calcifications in the right upper outer quadrant before NAT (arrows). (B) After NAT, microcalcifications increased (5.6 cm) (arrows). (C) MRI showing enhancing mass in the right breast (arrow). (D) After NAT, the right breast mass (arrow) decreased remarkably, and the postoperative pathological tumor size was observed to be 1.5 cm. NAT, neoadjuvant treatment; MRI, magnetic resonance imaging.

The correlation of pathological tumor size, extent of residual microcalcification on MG, and size of enhancing lesion on MRI

The median size of residual microcalcifications was 2.8 cm (IQR, 0.9–4.8), the median size of the residual tumor on MRI after NAT was 0.8 cm (IQR, 0–1.5), and the median total pathological size was 0.4 cm (IQR, 0–1.5). Overall, there was no correlation when comparing the agreement between pathologic tumor size and residual microcalcifications on MG (ICC =0.097) and a higher correlation with enhancing tumors on MRI (ICC =0.771). Furthermore, no significant association was found between the residual microcalcifications on MG and enhancing tumors on MRI (ICC =0.140). In the subgroup analysis for TN tumors, MRI enhancement showed the highest agreement with the size of the pathological residual tumor (ICC =0.883) (*Table 5*).

Discussion

We compared the accuracy of residual microcalcifications and MRI-enhanced lesions in assessing the residual tumor size in breast cancer after NAT. We found that MRI was more accurate than was MG in predicting the size of the pathological residual tumor and the NAT response. Meanwhile, we did not find a significant correlation

Table 4 Correlation of microcalcifications extent change on mammography after NAT with MRI radiologic reaction and histopathologic characteristics

Tumor response after NAT	Change in microcalcifications after NAT, n (%)			P value
	No change, n=56 (44.1)	Decrease, n=49 (38.6)	Increase, n=22 (17.3)	
RECIST criteria				0.09
Complete response (n=42)	22 (52.4)	15 (35.7)	5 (11.9)	
Partial response (n=70)	26 (37.1)	32 (45.7)	12 (17.1)	
Stable disease (n=15)	8 (53.3)	2 (13.3)	5 (33.3)	
Progressive disease (n=0)	–	–	–	
MP grade				0.14
1 (n=1)	1 (100.0)	0	0	
2 (n=8)	4 (50.0)	1 (12.5)	3 (37.5)	
3 (n=51)	18 (35.3)	20 (39.2)	13 (25.5)	
4 (n=15)	8 (53.3)	7 (46.7)	0	
5 (n=52)	25 (48.1)	21 (40.4)	6 (11.5)	
pCR				0.40
Yes (n=52)	25 (48.1)	21 (40.4)	6 (11.5)	
No (n=75)	31 (41.3)	28 (37.3)	16 (21.3)	
Postoperative pathological type				0.20
No residual cancer (n=32)	13 (40.6)	15 (46.9)	4 (12.5)	
Invasive carcinoma (n=65)	24 (36.9)	27 (41.5)	14 (21.5)	
IDC + DCIS (n=10)	7 (70.0)	1 (10.0)	2 (20.0)	
DCIS (n=20)	12 (60.0)	6 (30.0)	2 (10.0)	

NAT, neoadjuvant treatment; MP grade, Miller-Payne grade; pCR, pathologic complete response; IDC, invasive ductal carcinoma; DCIS, ductal carcinoma in situ; MRI, magnetic resonance imaging; RECIST, Response Evaluation Criteria in Solid Tumors.

between changes in the extent of the microcalcifications and pathologic response based on the MP grade and the RECIST criteria on MRI. Our results indicate that MRI could be considered an important auxiliary method for evaluating the pathological tumor size of breast cancer with residual microcalcifications, and it could provide surgeons with useful information for surgical decision-making.

Numerous studies have consistently demonstrated that, compared with MG and ultrasound, MRI has superior reliability in monitoring pathological response and evaluating residual tumor size (15-18). Surgeons' assessment of the tumor relies heavily on post-NAT imaging. However, the presence of microcalcifications after NAT may affect surgical decision-making. Previous studies have suggested that changes in microcalcifications are associated with pCR (7,19). Patients with a decrease in the extent of microcalcifications post-NAT have higher rates of pCR than those with no change or an increased extent. In contrast to prior investigations, our study included patients who underwent both pre- and post-NAT MRI scans, enabling us to not only evaluate the correlation between microcalcification changes and pathological response but also to examine their association with radiological response based on MRI. Interestingly, we did not observe a significant relationship between changes in microcalcifications and pathological response as determined by the MP grade and RECIST criteria on MRI (P=0.09 and P=0.14, respectively). Li *et al.* concluded that mammographically detected calcifications had no predictive value for tumor response after NAT (20). Most studies have reported that microcalcifications may remain unchanged, decrease, or even increase in patients after NAT

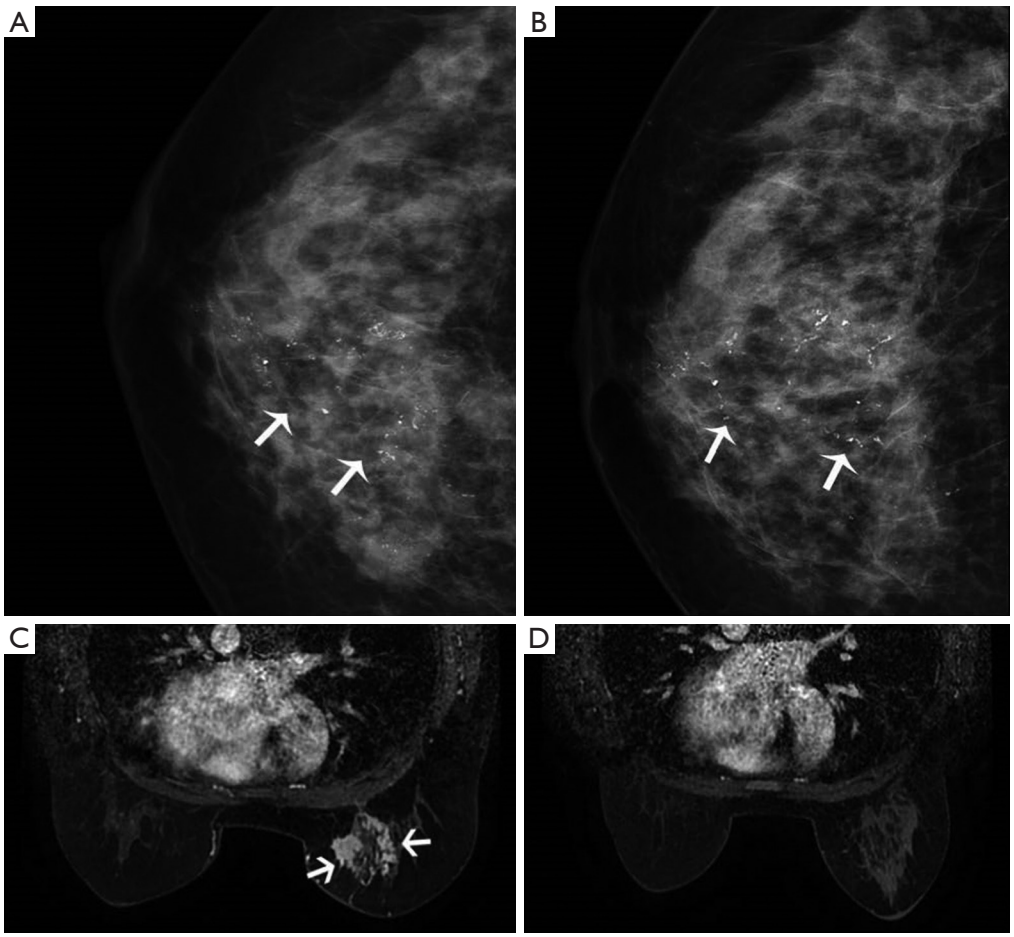

Figure 3 Imaging of a 52-year-old woman with invasive ductal carcinoma. (A) Mammogram showing fine linear segmental calcifications (8.6 cm) in the right upper inner quadrant before NAT (arrows). (B) No obvious changes in the size of calcifications after NAT (arrows). (C) MRI showing multiple enhancing masses in the right breast (arrows). (D) Lesions on MRI disappeared, and final pathology confirmed complete resolution. NAT, neoadjuvant treatment; MRI, magnetic resonance imaging.

(21,22). The persistence of calcification does not invariably indicate the presence of residual tumors (23). The decrease and disappearance of microcalcifications may be attributed to the phagocytosis of multinucleated histiocytes or partial removal via biopsy, while the necrotic process of carcinomas can be accompanied by calcification formation, which may account for the increased degree of calcification in some patients (24,25). Previous studies have reported microcalcifications in 60–90% of cases of DCIS (26), but our study did not find a significant increase in calcification in postoperative pathological types of invasive carcinomas with or without DCIS. This observation may be attributed to the limited sample size in our study.

In our study, we found that the total residual tumor sizes on MRI showed higher agreement with the actual tumor sizes on histopathologic examination than with the extent of residual microcalcifications on MG (ICC: 0.771 *vs.* 0.097). The reliability of MRI for the prediction of residual tumors was highest for the TN subtype (ICC =0.883). Notably, MRI exhibited the highest reliability in predicting residual tumors within the TN subtype (ICC =0.883). These findings align with those reported by Kim *et al.*, who also found moderate agreement between MRI and residual microcalcifications on MG in predicting the extent of residual tumors across all subtypes (ICC: 0.709 *vs.* 0.365) (27). In our study, MRI demonstrated a high sensitivity and PPV in evaluating whether breast cancer achieved pCR, with a low false-negative rate. However,

Table 5 The correlation between pathological tumor size, the extent of residual microcalcification on MG, and size of enhancing lesion on MRI

Molecular subtype	Extent of residual microcalcifications on MG (cm), median (IQR)	Size of enhancing lesion on MRI (cm), median (IQR)	Size of residual tumor (cm), median (IQR)	ICC[a] (95% CI)	ICC[b] (95% CI)	ICC[c] (95% CI)
Total (n=127)	2.8 (0.9 to 4.8)	0.8 (0 to 1.5)	0.4 (0 to 1.5)	0.097 (–0.078 to 0.266)	0.771 (0.689 to 0.833)	0.140 (–0.035 to 0.306)
HR–/HER2+ (n=25)	3.7 (2.0 to 5.2)	0 (0 to 1.0)	0 (0 to 0.2)	0.161 (–0.243 to 0.517)	0.757 (0.522 to 0.885)	0.082 (–0.316 to 0.456)
HR+/HER2+ (n=42)	2.9 (1.0 to 4.5)	0.6 (0 to 1.1)	0.2 (0 to 1.5)	0.134 (–0.174 to 0.418)	0.717 (0.531 to 0.837)	0.149 (–0.159 to 0.430)
HR+/HER2– (n=47)	2.4 (0.6 to 4.7)	1.2 (0.6 to 2.2)	1.2 (0.5 to 2.5)	0.175 (–0.118 to 0.441)	0.736 (0.570 to 0.844)	0.255 (–0.032 to 0.503)
TN (n=13)	2.8 (1.5 to 6.1)	1.0 (0.3 to 1.7)	0.8 (0 to 1.6)	–0.018 (–0.545 to 0.519)	0.883 (0.662 to 0.963)	0.065 (–0.484 to 0.577)

[a], ICC between the extent of residual microcalcifications on MG and histopathology; [b], ICC between the extent of enhancing lesion on MRI and histopathology; [c], ICC between the extent of residual microcalcifications on MG and enhancing lesion on MRI. MG, mammography; MRI, magnetic resonance imaging; IQR, interquartile range; ICC, intraclass correlation coefficient; CI, confidence interval; HR, hormone receptor; HER2, human epidermal growth factor receptor 2; TN, triple negative.

we observed some variations in the accuracy of MRI in assessing treatment responses among different tumor types. Specifically, 6 patients with ER-positive tumors were misdiagnosed as having achieved complete response on MR, despite the presence of invasive residual tumor on pathology. This discrepancy may be attributed to the tendency of ER-positive tumors to exhibit scattered small lesions following NAT (28).

BCS offers several advantages, including minimal incision, reduced intraoperative blood loss, and favorable cosmetic outcomes, all of which contribute to a higher quality of life for patients (29-31). Previous studies have indicated that patients undergoing BCS exhibit comparable or even improved survival rates compared to those who undergo mastectomy (32-34).

Some clinicians advocate for the complete removal of microcalcifications seen in MG, while others argue that if the tumor demonstrates significant shrinkage or achieves pCR, the removal of all microcalcifications may not be required (20,24,35). We suggest that residual tumors with microcalcifications may not necessarily be a contraindication to breast conservation. In our study, 81% of patients opted for the mastectomy after NAT, nearly 40% of whom had pCR. Additionally, only 23% of BCS-eligible patients chose BCS after NAT, representing a significantly lower BCS rate than in North American patients (55%) (36). These results provide valuable insights for surgeons in making informed decisions regarding the appropriate surgical approach. It is possible that not all lesions exhibiting persistent microcalcifications require more extensive surgical interventions.

This study had several limitations. First, this was a single-center study with a relatively small sample size. Second, the patients included in the study were treated with diverse neoadjuvant regimens and varied treatment cycles prior to surgery. Additionally, there was no postoperative follow-up conducted for our patients.

Conclusions

Our findings indicate that in patients with persistent microcalcifications after NAT, clinicians should evaluate both MRI findings and immunohistochemical subtypes and should consider the feasibility of BCS when deciding on surgery. Further investigations with larger prospective cohorts are required to verify these results.

Acknowledgments

Funding: This work was supported by the Key R&D Program of Guangdong Province (No. 2021B0101420006), the National Science Fund for Distinguished Young Scholars (No. 81925023), the National Science Foundation for Young Scientists of China (Nos. 81701662 and 82102019), the National Natural Science Foundation of China (Nos. 62002082, 82071892, 82171920, and

12126610), and the Guangdong Provincial Key Laboratory of Artificial Intelligence in Medical Image Analysis and Application (No. 2022B1212010011).

Footnote

Reporting Checklist: The authors have completed the STROBE reporting checklist. Available at https://qims.amegroups.com/article/view/10.21037/qims-22-1170/rc

Conflicts of Interest: All authors have completed the ICMJE uniform disclosure form (available at https://qims.amegroups.com/article/view/10.21037/qims-22-1170/coif). The authors have no conflicts of interest to declare.

Ethical Statement: The authors are accountable for all aspects of the work in ensuring that questions related to the accuracy or integrity of any part of the work are appropriately investigated and resolved. The study was conducted in accordance with the Declaration of Helsinki (as revised in 2013) and was approved by the Research Ethics Committee of Guangdong Provincial People's Hospital. Individual consent for this retrospective analysis was waived.

References

1. Sung H, Ferlay J, Siegel RL, Laversanne M, Soerjomataram I, Jemal A, Bray F. Global Cancer Statistics 2020: GLOBOCAN Estimates of Incidence and Mortality Worldwide for 36 Cancers in 185 Countries. CA Cancer J Clin 2021;71:209-49.
2. Cox RF, Hernandez-Santana A, Ramdass S, McMahon G, Harmey JH, Morgan MP. Microcalcifications in breast cancer: novel insights into the molecular mechanism and functional consequence of mammary mineralisation. Br J Cancer 2012;106:525-37.
3. Tabár L, Vitak B, Chen TH, Yen AM, Cohen A, Tot T, Chiu SY, Chen SL, Fann JC, Rosell J, Fohlin H, Smith RA, Duffy SW. Swedish two-county trial: impact of mammographic screening on breast cancer mortality during 3 decades. Radiology 2011;260:658-63.
4. Mordang JJ, Gubern-Mérida A, Bria A, Tortorella F, Mann RM, Broeders MJM, den Heeten GJ, Karssemeijer N. The importance of early detection of calcifications associated with breast cancer in screening. Breast Cancer Res Treat 2018;167:451-8.
5. Steenbruggen TG, van Ramshorst MS, Kok M, Linn SC, Smorenburg CH, Sonke GS. Neoadjuvant Therapy for Breast Cancer: Established Concepts and Emerging Strategies. Drugs 2017;77:1313-36.
6. von Minckwitz G, Untch M, Blohmer JU, Costa SD, Eidtmann H, Fasching PA, Gerber B, Eiermann W, Hilfrich J, Huober J, Jackisch C, Kaufmann M, Konecny GE, Denkert C, Nekljudova V, Mehta K, Loibl S. Definition and impact of pathologic complete response on prognosis after neoadjuvant chemotherapy in various intrinsic breast cancer subtypes. J Clin Oncol 2012;30:1796-804.
7. Golan O, Amitai Y, Menes T. Does change in microcalcifications with neoadjuvant treatment correlate with pathological tumour response? Clin Radiol 2016;71:458-63.
8. Feliciano Y, Mamtani A, Morrow M, Stempel MM, Patil S, Jochelson MS. Do Calcifications Seen on Mammography After Neoadjuvant Chemotherapy for Breast Cancer Always Need to Be Excised? Ann Surg Oncol 2017;24:1492-8.
9. Breast Cancer NCCN Evidence Blocks. Version 3.2022. Accessed May 14, 2022. Availble online: https://www.nccn.org/
10. Um E, Kang JW, Lee S, Kim HJ, Yoon TI, Sohn G, Chung IY, Kim J, Lee JW, Son BH, Ahn SH, Ko BS. Comparing Accuracy of Mammography and Magnetic Resonance Imaging for Residual Calcified Lesions in Breast Cancer Patients Undergoing Neoadjuvant Systemic Therapy. Clin Breast Cancer 2018;18:e1087-91.
11. Spak DA, Plaxco JS, Santiago L, Dryden MJ, Dogan BE. BI-RADS(®) fifth edition: A summary of changes. Diagn Interv Imaging 2017;98:179-90.
12. Lai YC, Chang WC, Chen CB, Wang CL, Lin YF, Ho MM, Cheng CY, Huang PW, Hsu CW, Lin G. Response evaluation for immunotherapy through semi-automatic software based on RECIST 1.1, irRC, and iRECIST criteria: comparison with subjective assessment. Acta Radiol 2020;61:983-91.
13. Spitale A, Mazzola P, Soldini D, Mazzucchelli L,

Bordoni A. Breast cancer classification according to immunohistochemical markers: clinicopathologic features and short-term survival analysis in a population-based study from the South of Switzerland. Ann Oncol 2009;20:628-35.
14. Ogston KN, Miller ID, Payne S, Hutcheon AW, Sarkar TK, Smith I, Schofield A, Heys SD. A new histological grading system to assess response of breast cancers to primary chemotherapy: prognostic significance and survival. Breast 2003;12:320-7.
15. Amitai Y, Scaranelo A, Menes TS, Fleming R, Kulkarni S, Ghai S, Freitas V. Can breast MRI accurately exclude malignancy in mammographic architectural distortion? Eur Radiol 2020;30:2751-60.
16. Rauch GM, Adrada BE, Kuerer HM, van la Parra RF, Leung JW, Yang WT. Multimodality Imaging for Evaluating Response to Neoadjuvant Chemotherapy in Breast Cancer. AJR Am J Roentgenol 2017;208:290-9.
17. Lobbes MB, Prevos R, Smidt M, Tjan-Heijnen VC, van Goethem M, Schipper R, Beets-Tan RG, Wildberger JE. The role of magnetic resonance imaging in assessing residual disease and pathologic complete response in breast cancer patients receiving neoadjuvant chemotherapy: a systematic review. Insights Imaging 2013;4:163-75.
18. He M, Su J, Ruan H, Song Y, Ma M, Xue F. Nomogram based on quantitative dynamic contrast-enhanced magnetic resonance imaging, apparent diffusion coefficient, and clinicopathological features for early prediction of pathologic complete response in breast cancer patients receiving neoadjuvant chemotherapy. Quant Imaging Med Surg 2023;13:4089-102.
19. Yim H, Ha T, Kang DK, Park SY, Jung Y, Kim TH. Change in microcalcifications on mammography after neoadjuvant chemotherapy in breast cancer patients: correlation with tumor response grade and comparison with lesion extent. Acta Radiol 2019;60:131-9.
20. Li JJ, Chen C, Gu Y, Di G, Wu J, Liu G, Shao Z. The role of mammographic calcification in the neoadjuvant therapy of breast cancer imaging evaluation. PLoS One 2014;9:e88853.
21. Weiss A, Lee KC, Romero Y, Ward E, Kim Y, Ojeda-Fournier H, Einck J, Blair SL. Calcifications on mammogram do not correlate with tumor size after neoadjuvant chemotherapy. Ann Surg Oncol 2014;21:3310-6.
22. Kim EY, Do SI, Yun JS, Park YL, Park CH, Moon JH, Youn I, Choi YJ, Ham SY, Kook SH. Preoperative evaluation of mammographic microcalcifications after neoadjuvant chemotherapy for breast cancer. Clin Radiol 2020;75:641.e19-27.
23. Esserman LE, d'Almeida M, Da Costa D, Gerson DM, Poppiti RJ Jr. Mammographic appearance of microcalcifications: can they change after neoadjuvant chemotherapy? Breast J 2006;12:86-7.
24. Goldberg H, Zandbank J, Kent V, Leonov-Polak M, Livoff A, Chernihovsky A, Guindy M, Evron E. Chemotherapy may eradicate ductal carcinoma in situ (DCIS) but not the associated microcalcifications. Eur J Surg Oncol 2017;43:1415-20.
25. Vanna R, Morasso C, Marcinnò B, Piccotti F, Torti E, Altamura D, Albasini S, Agozzino M, Villani L, Sorrentino L, Bunk O, Leporati F, Giannini C, Corsi F. Raman Spectroscopy Reveals That Biochemical Composition of Breast Microcalcifications Correlates with Histopathologic Features. Cancer Res 2020;80:1762-72.
26. Rauch GM, Hobbs BP, Kuerer HM, Scoggins ME, Benveniste AP, Park YM, Caudle AS, Fox PS, Smith BD, Adrada BE, Krishnamurthy S, Yang WT. Microcalcifications in 1657 Patients with Pure Ductal Carcinoma in Situ of the Breast: Correlation with Clinical, Histopathologic, Biologic Features, and Local Recurrence. Ann Surg Oncol 2016;23:482-9.
27. Kim YS, Chang JM, Moon HG, Lee J, Shin SU, Moon WK. Residual Mammographic Microcalcifications and Enhancing Lesions on MRI After Neoadjuvant Systemic Chemotherapy for Locally Advanced Breast Cancer: Correlation with Histopathologic Residual Tumor Size. Ann Surg Oncol 2016;23:1135-42.
28. Ko ES, Han BK, Kim RB, Ko EY, Shin JH, Hahn SY, Nam SJ, Lee JE, Lee SK, Im YH, Park YH. Analysis of factors that influence the accuracy of magnetic resonance imaging for predicting response after neoadjuvant chemotherapy in locally advanced breast cancer. Ann Surg Oncol 2013;20:2562-8.
29. Jagsi R, Li Y, Morrow M, Janz N, Alderman A, Graff J, Hamilton A, Katz S, Hawley S. Patient-reported Quality of Life and Satisfaction With Cosmetic Outcomes After Breast Conservation and Mastectomy With and Without Reconstruction: Results of a Survey of Breast Cancer Survivors. Ann Surg 2015;261:1198-206.
30. Wang Z, Han X. Clinical significance of breast-conserving surgery for early breast cancer and its impact on patient life quality of life. J BUON 2019;24:1898-904.
31. Kim MK, Kim T, Moon HG, Jin US, Kim K, Kim J, Lee JW, Kim J, Lee E, Yoo TK, Noh DY, Minn KW, Han W. Effect of cosmetic outcome on quality of life after breast

cancer surgery. Eur J Surg Oncol 2015;41:426-32.
32. Veronesi U, Cascinelli N, Mariani L, Greco M, Saccozzi R, Luini A, Aguilar M, Marubini E. Twenty-year follow-up of a randomized study comparing breast-conserving surgery with radical mastectomy for early breast cancer. N Engl J Med 2002;347:1227-32.
33. Hartmann-Johnsen OJ, Kåresen R, Schlichting E, Nygård JF. Survival is Better After Breast Conserving Therapy than Mastectomy for Early Stage Breast Cancer: A Registry-Based Follow-up Study of Norwegian Women Primary Operated Between 1998 and 2008. Ann Surg Oncol 2015;22:3836-45.
34. Agarwal S, Pappas L, Neumayer L, Kokeny K, Agarwal J. Effect of breast conservation therapy vs mastectomy on disease-specific survival for early-stage breast cancer. JAMA Surg 2014;149:267-74.
35. Li Y, Cao J, Zhou Y, Mao F, Shen S, Sun Q. Mammographic casting-type calcification is an independent prognostic factor in invasive breast cancer. Sci Rep 2019;9:10544.
36. Golshan M, Loibl S, Wong SM, Houber JB, O'Shaughnessy J, Rugo HS, Wolmark N, McKee MD, Maag D, Sullivan DM, Metzger-Filho O, Von Minckwitz G, Geyer CE Jr, Sikov WM, Untch M. Breast Conservation After Neoadjuvant Chemotherapy for Triple-Negative Breast Cancer: Surgical Results From the BrighTNess Randomized Clinical Trial. JAMA Surg 2020;155:e195410.

Cite this article as: Zhu C, Chen M, Liu Y, Li P, Ye W, Ye H, Ye Y, Liu Z, Liang C, Liu C. Value of mammographic microcalcifications and MRI-enhanced lesions in the evaluation of residual disease after neoadjuvant therapy for breast cancer. Quant Imaging Med Surg 2023;13(9):5593-5604. doi: 10.21037/qims-22-1170

